Enrichment of Cysteine S-palmitoylation using Sodium Deoxycholate Acid Precipitation - SDC-ACE

Peter T. Jensen and Martin R. Larsen*

Protein Research Group, Department of Biochemistry and Molecular Biology, University of Southern Denmark, 5230 Odense M, Denmark.

***Corresponding Author: Prof. Dr. Martin R. Larsen:**

Department of Biochemistry and Molecular Biology, the University of Southern Denmark, Denmark.

Phone.: 45-60-111872; E-mail: mrl@bmb.sdu.dk

Abstract

Protein S-palmitoylation is an important post-translational modification regulating biological pathways for broad cell function. We describe a simple and fast approach to identify cysteine S-palmitoylation. We applied the method to S-palmitoylation in the mouse brain, identifying more than 6600 putative S-palmitoylated proteins, including many well-characterized S-palmitoylated proteins, linking S-palmitoylation to both membrane association and to protein complex assembly.

Main

Protein lipidation is the covalent attachment of lipid molecules to proteins. It enables dynamic protein modulation by changing binding affinities, stability, folding, location, and interaction [1]. It is involved in many cellular processes, including trafficking, migration and cell signaling, and is associated with different human diseases[1, 2].

Cysteine S-palmitoylation, also referred to as S-acetylation, is the most common lipid modification, adding a palmitate moiety onto cysteines[1, 3]. S-palmitoylation is a reversible protein lipid modification, allowing for dynamic modulation of protein function and location[1]. It is catalyzed by zDHHC S-acyltransferases, a family of 23 or 24 genes in mammals[3]. The enzymes are membrane associated and contain a highly conserved aspartate-histidine-histidine-cysteine (DHHC) motif within a zinc-binding domain [3].

Techniques for studying S-palmitoylation are affinity based, such as acyl-biotin exchange (ABE) or acyl-resin assisted capture (Acyl-RAC) and metabolic-labelling [1]. ABE relies on alkylation of free cysteines, followed by removal of S-palmitoylation using hydroxylamine (HA), then reacting newly freed cysteine thiol groups with biotin. The formerly S-palmitoylated peptides are enriched on streptavidin-beads. For Acyl-RAC the HA released formerly S-palmitoylated peptides are captured using thiopropyl Sepharose beads [1]. Metabolic approaches use bio-orthogonal probes like 17-octadecyonic acid (17-ODYA) to label palmitoylation sites, followed by click chemistry to identify the labelled sites [1].

We present a simple and fast method for enriching formerly S-palmitoylated peptides using sodium deoxycholate (SDC) liquid-solid separation combined with dithiothreitol (DTT) reduction and acid precipitation, termed SDC Acid S-Palmitoylated Peptide Enrichment (SDC-ACE). We optimized the method on synthetic S-palmitoylated peptides and applied it to identify protein S-palmitoylation in the mouse brain.

SDC is a frequently used detergent in proteomics, since proteases, such as trypsin, retain activity in SDC[4] and it is easily removed with acid precipitation and centrifugation. However, acid precipitation results in a loss of peptides to the SDC pellet (Supplementary fig. S1A). Repeated

washing of the SDC pellet by re-solubilization in pH 8-8.5 buffer followed by acid precipitation, resulted in recovery of primarily hydrophobic peptides in the last washes (Supplementary fig. S1B). This together with the relatively large amount of remaining material in the SDC pellet judged from the nanodrop (280 nm), indicating that hydrophobic peptides bind tightly to precipitated SDC. We therefore hypothesized that lipid modified peptides are enriched in the SDC pellet.

To test this, three synthetic S-palmitoylated peptides (sequence A, B and C) [5] were generated (Supplementary fig. S2A-C), as S-palmitoylation can be reduced using various reducing reagents. To test if S-palmitoylation peptides co-precipitate with the SDC after acidification and centrifugation, the three S-palmitoylated peptides (A-, B-, and C-Palm) were combined and analyzed by MALDI-MS (Fig 1Aa). SDC was added to the mixture to a final concentration of 1% w/v followed by acidification and centrifugation. MALDI-MS analysis of the supernatant revealed their complete removal (Fig. 1Ab), indicating efficient enrichment of the S-palmitoylated peptides with SDC acidic precipitation.

The three peptides were incubated with common reagents used for reduction and release of S-palmitoylation; Tris(2-carboxyethyl)phosphine (TCEP), DTT and HA, to test efficiency in releasing the S-palmitoylation. Despite that HA is used in most strategies for enrichment of formerly S-palmitoylated peptides, its ability to reduce abundant disulfide bonds is problematic in these strategies (see Note 1). The S-palmitoylated peptides were incubated with different concentrations of HA, DTT and TCEP for 60 min and de-palmitoylated peptides were quantified using LC-MSMS (Fig. 1B). Surprisingly, HA (100 mM) resulted in a small increase of peptide de-palmitoylation compared to 750 mM or 1000 mM, despite that 100 mM HA is frequently used as control in ABE and Acyl-RAC. DTT was the most efficient of the three de-palmitoylation methods. We choose 20 mM DTT as the optimum DTT concentration for release of de-palmitoylation peptides from the SDC pellet since this concentration show efficient de-palmitoylation and does not require high concentration of subsequent alkylating reagent (Supplementary fig. S3).

The specificity of the SDC enrichment of the S-palmitoylation peptides in a background of peptides derived from bovine lactoglobulin was examined by MALDI-MS analysis (Fig. 1Ca-c). After adding SDC to 1% followed by acidic precipitation and centrifugation, the supernatant (S1) was analyzed and signals originating from the S-palmitoylated peptides were absent, suggesting association with the SDC (Fig. 1Cd). Washing the precipitated SDC pellet only recovered remnant peptides from lactoglobulin as expected (Fig. 1Ce). Resuspending the pellet and de-palmitoylated using 20 mM DTT resulted in the selective release of all three de-palmitoylated peptides (Fig. 1Cf), illustrating high selectivity of the method.

We designed the overall SDC-ACE strategy for enriching formerly S-palmitoylated peptides using SDC acid precipitation to be applied to cells and tissues (Fig. 1D). Proteins are first extracted using 3-10% SDC (better analysis is obtained using a crude membrane preparation[6]), reduced using 1-3 mM TCEP and alkylated using 10 mM N-ethylmaleimide. The proteins are then proteolyzed using trypsin. The digest is acidified and the SDC pellet is washed 3 times with buffer 1 and twice with H_2O. Finally, reduction of S-palmitoylation is performed using DTT and subsequent alkylation of de-palmitoylated cysteines using Iodoacetamide. De-palmitoylated peptides are collected from the supernatant following SDC acid precipitation and analyzed by 1D or 2D LC-MSMS. A small volume of SDC sample without DTT serves as an MS background control for the de-palmitoylation step (Supplementary fig. S4).

The SDC-ACE method was applied to a crude membrane preparation from mouse brain in replicates using a total of 2 mg protein as starting material. From the replicates 36,072 unique cysteine-containing peptides (Supplementary table S1-3) were obtained from 6,632 proteins (Fig. 2A). A small aliquot of the SDC pellet analyzed with and without DTT revealed a “false discovery rate” below 0.49% (Supplementary fig. S4). A total of 81.6% of the peptides contained one cysteine, whereas 18.4% of the peptides contained two or more closely spaced cysteines mostly in disordered regions, generating highly hydrophobic protein surfaces for interaction with lipid membranes (Fig. 2.A).

This data identified 1,999 of the 3,882 known or predicted unique S-palmitoylation sites in the mouse SwissPalm database[7] (51.49%), including 67 of the only 213 validated unique sites in the database (Fig. 2B). Some of the validated sites were not identified due to the tryptic cleavage specificity.

A total of 1,369 peptides from 768 proteins contained 3 or more cysteines located in the same peptide, indicating hydrophobic clusters (Fig. 2A). Pathway analysis found these proteins to associate with ECM receptor signaling, focal adhesion and synaptic membranes, as well as with membrane associated proteins such as Metallothionin (MT) proteins involved in cellular zinc ion homeostasis (Fig. 2C). The function of proteins containing peptides with single and double S-palmitoylation sites was highly associated with known larger protein complexes, such as the ribosome, spliceosome, proteosome, COPII-complex, Exocyst complex, mTOR-complex 1, Complex I-V and ATPase Complexes (mitochondrial respiratory system) (Fig 2C). S-palmitoylation has previously been associated with some of these complexes[7-10], however, the results strongly suggest that S-palmitoylation may be of much broader importance for formation, interaction and regulation of protein complexes and protein-protein interaction in the cell.

Among the 32 proteins of the nuclear pore complex[11, 12] S-palmitoylation sites were identified on 25, suggesting that S-palmitoylation may be central to cytoplasmic - nuclear transport (Supplementary fig. S5). Furthermore, S-palmitoylation sites were identified on 16 out of the 23 palmitoyl-transferases, on more than 90 E3 ubiquitin-protein ligases and on more than 200 protein kinases, suggesting that this modification may be considerably more abundant on regulatory proteins than previously believed.

Many well-known S-palmitoylated proteins were identified, such as Snap25a/b (annotated spectra for the de-palmitoylated peptides in Supplementary fig. S6A and S6B), involved in the SNARE complex involved in synaptic vesicle exocytosis and PSD-95, a postsynaptic scaffolding protein required for synaptic plasticity[13]. A peptide from the N-terminal of restriction factor Serine incorporator 5 was identified containing 10 de-palmitoylated sites in a single peptide (Supplementary fig. S7).

The new SDC-ACE method is an efficient and easy method for identification of S-palmitoylation sites. It is associated with less false identifications due to the efficient enrichment of the S-palmitoylated peptides with SDC prior to de-palmitoylation and the elimination of the use of hydroxylamine, which was here found to reduce abundant disulfide bonds at high concentrations resulting in false identifications.

Figure 1

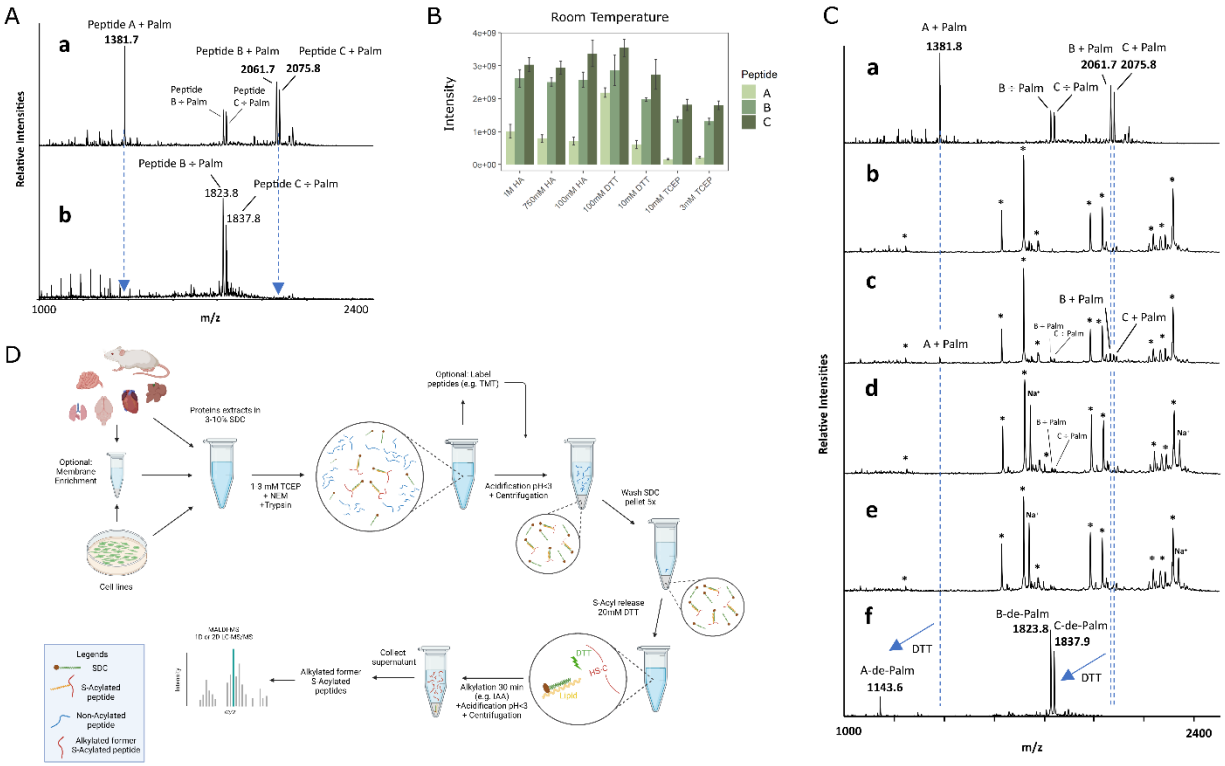

Figure 1: Development of a method for efficient enrichment of S-acylated peptides. *A) (a) MALDI MS analysis of synthetic S-palmitoylated peptides (b) MALDI MS analysis of supernatant after SDC precipitation B) Analysis of the most efficient reagent for releasing S-palmitoylation. DTT was comparably more efficient at releasing S-palmitoylation compared to HA and TCEP. C) Specificity of our method demonstrated by mixing synthetic S-palmitoylated peptides (a) with lactoglobulin derived peptides (b). The mix of peptides (c) shows both lactoglobulin peptides (*) and Palm/÷Palm peptides. S-palmitoylated peptides are retained in the SDC pellet as shown from precipitation and washing supernatants (d-e). (f) efficient release of de-palmitoylated peptides from the SDC fraction using DTT. D) Schematic representation of the SDC-ACE workflow using SDC acid precipitation for efficient S-palmitoylated peptide enrichment. Schematic representation was created with BioRender.com.*

Figure 2

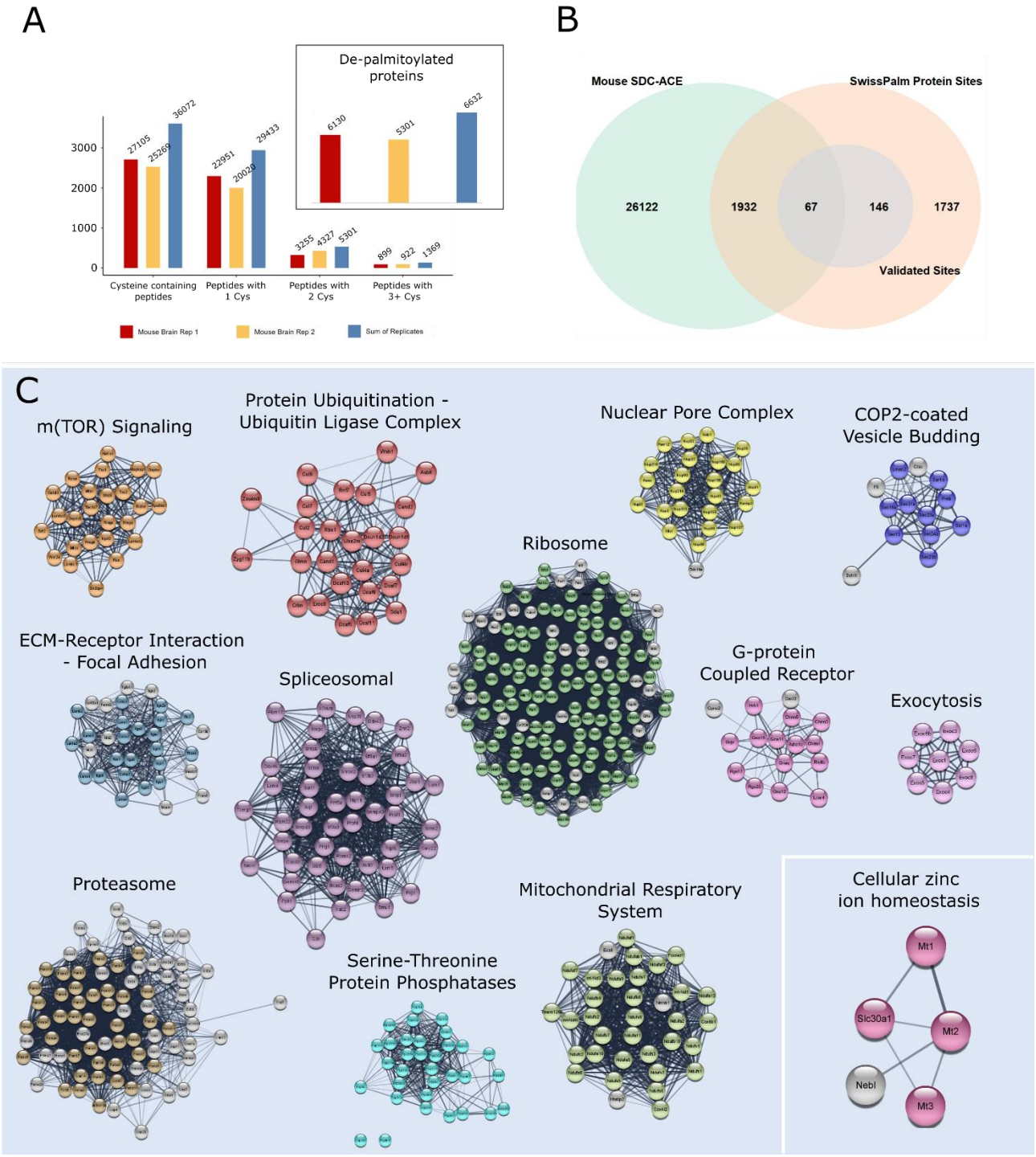

Figure 2: Enriched S-palmitoylation from mouse brain samples. *A) The number of identified peptides and proteins in each replicate and the sum of both. Peptides are separated based on number of S-palmitoylation modifications, ranging from one to 3+. B) Comparison of enriched mouse brain S-palmitoylation with all unique S-palmitoylated peptide sites and all validated unique sites in the SwissPalm database. C) Functional enrichment of GO and KEGG-pathway terms of the enriched mouse brain protein S-palmitoylation using Cytoscape StringApp[14, 15].*

References

1. Main, A. and W. Fuller, *Protein S-Palmitoylation: advances and challenges in studying a therapeutically important lipid modification.* FEBS J, 2022. **289**(4): p. 861-882.
2. Dong, G., et al., *Palmitoylation couples insulin hypersecretion with beta cell failure in diabetes.* Cell Metab, 2023. **35**(2): p. 332-344 e7.
3. Malgapo, M.I.P. and M.E. Linder, *Substrate recruitment by zDHHC protein acyltransferases.* Open Biol, 2021. **11**(4): p. 210026.
4. Lin, Y., et al., *Sodium-deoxycholate-assisted tryptic digestion and identification of proteolytically resistant proteins.* Anal Biochem, 2008. **377**(2): p. 259-66.
5. Yousefi-Salakdehm, E., J. Johansson, and R. Strömberg, *A method for S- and O-palmitoylation of peptides synthesis of pulmonary surfactant protein-C models.* Biochem J. , 1999. **343**: p. 557-562.
6. Palmisano, G., et al., *Selective enrichment of sialic acid-containing glycopeptides using titanium dioxide chromatography with analysis by HILIC and mass spectrometry.* Nat Protoc, 2010. **5**(12): p. 1974-82.
7. Blanc, M., et al., *SwissPalm: Protein Palmitoylation database.* F1000Res, 2015. **4**: p. 261.
8. Virlogeux, A., et al., *Increasing brain palmitoylation rescues behavior and neuropathology in Huntington disease mice.* Science Advances, 2021. **7**(14).
9. Shen, L.F., et al., *Role of S-Palmitoylation by ZDHHC13 in Mitochondrial function and Metabolism in Liver.* Sci Rep, 2017. **7**(1): p. 2182.
10. Sanders, S.S., F.I. De Simone, and G.M. Thomas, *mTORC1 Signaling Is Palmitoylation-Dependent in Hippocampal Neurons and Non-neuronal Cells and Involves Dynamic Palmitoylation of LAMTOR1 and mTOR.* Front Cell Neurosci, 2019. **13**: p. 115.
11. Lin, D.H., et al., *Architecture of the symmetric core of the nuclear pore.* Science, 2016. **352**(6283): p. aaf1015.
12. Lin, D.H. and A. Hoelz, *The Structure of the Nuclear Pore Complex (An Update).* Annu Rev Biochem, 2019. **88**: p. 725-783.
13. Chen, B., et al., *Protein Lipidation in Cell Signaling and Diseases: Function, Regulation, and Therapeutic Opportunities.* Cell Chem Biol, 2018. **25**(7): p. 817-831.
14. Doncheva, N.T., et al., *Cytoscape StringApp: Network Analysis and Visualization of Proteomics Data.* J Proteome Res, 2019. **18**(2): p. 623-632.
15. Shannon, P., et al., *Cytoscape: a software environment for integrated models of biomolecular interaction networks.* Genome Res, 2003. **13**(11): p. 2498-504.

Supplementary

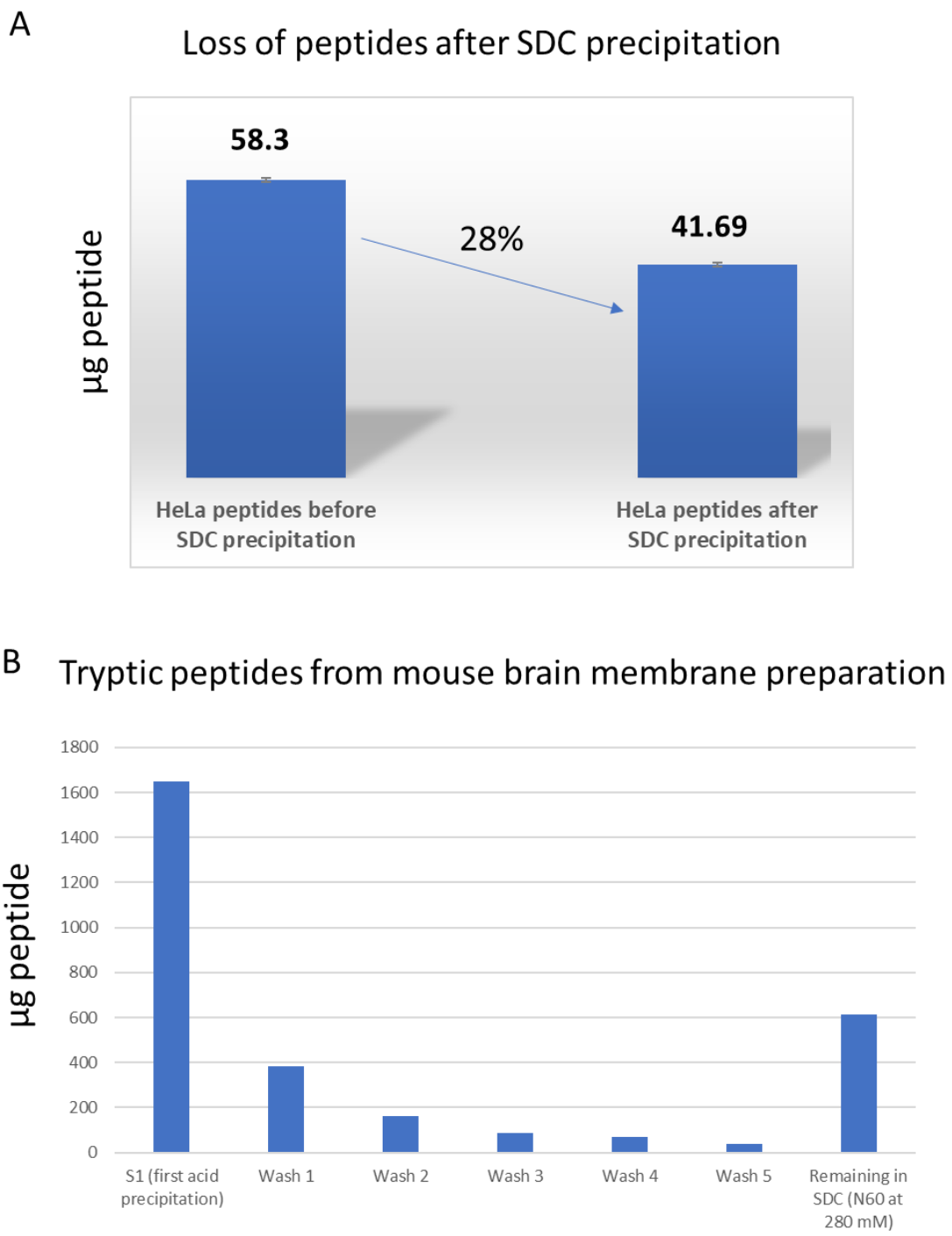

Figure S1: SDC acid precipitation of HeLa cells and mouse brain membrane preparation. *A) An aliquot corresponding to 58.3 µg of peptides originating from tryptic digestion of a HeLa cell lysate was taken out and added SDC to a total of 1% SDC. After SDC acid precipitation a loss of 28% of the peptides was lost in the SDC pellet. Amounts of peptides was determined by amino acid composition analysis (AAA). B) Proteins from a mouse brain membrane preparation was digested with trypsin in 5% SDC. The figure show the amounts of peptides present in the first acid precipitation (S1), the 5 subsequent washes (see methods), and the final solubilized SDC pellet. The peptide/protein was measured by nanodrop at 280 nm.*

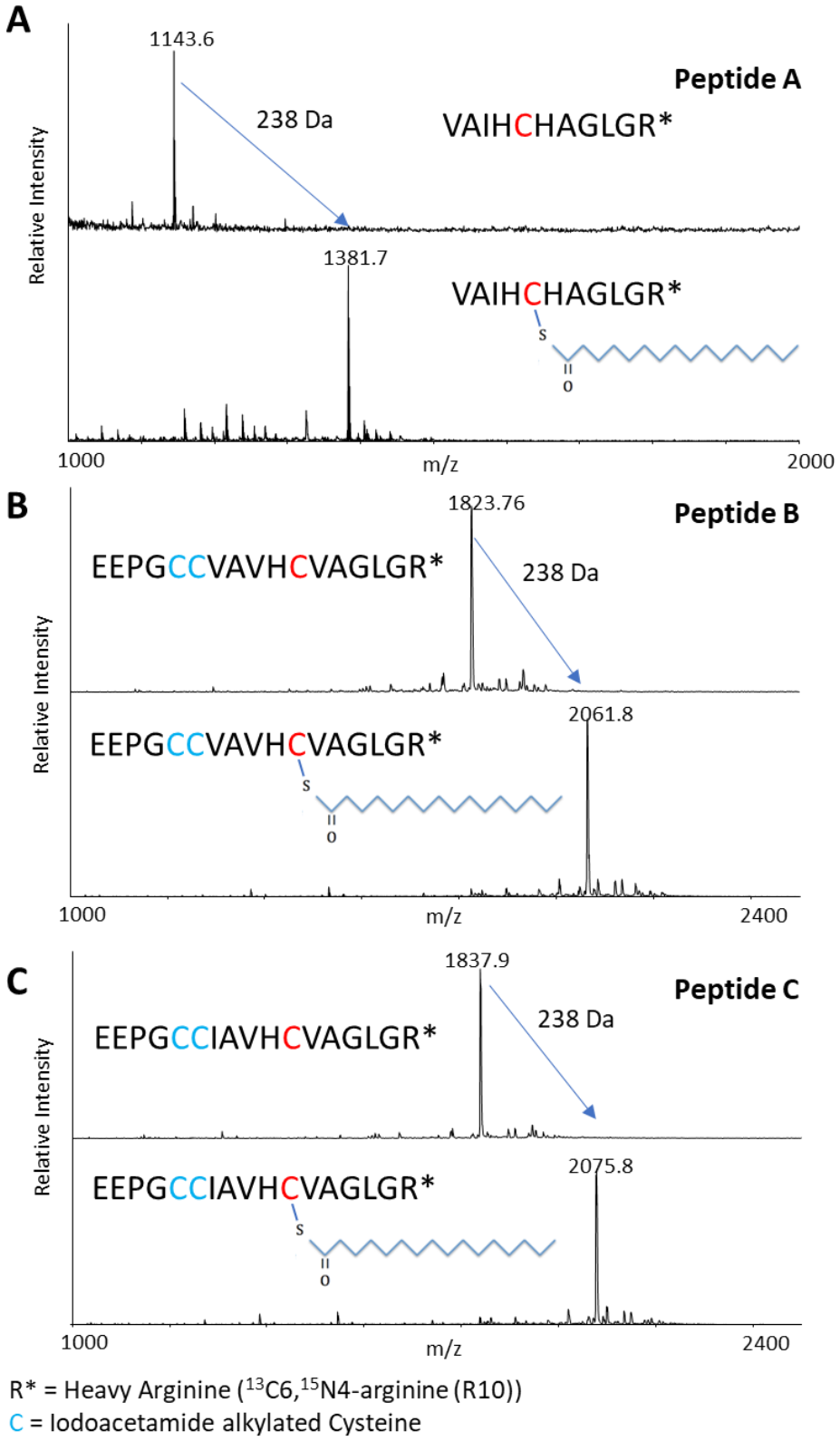

Figure S2: MALDI-MS analysis of palmitoylated synthetic peptides. *MALDI-MS spectra showing three synthetic peptides (A-C) before and after the S-palmitoylation reaction, resulting in an increase in 238 Da for each cysteine-containing peptide.*

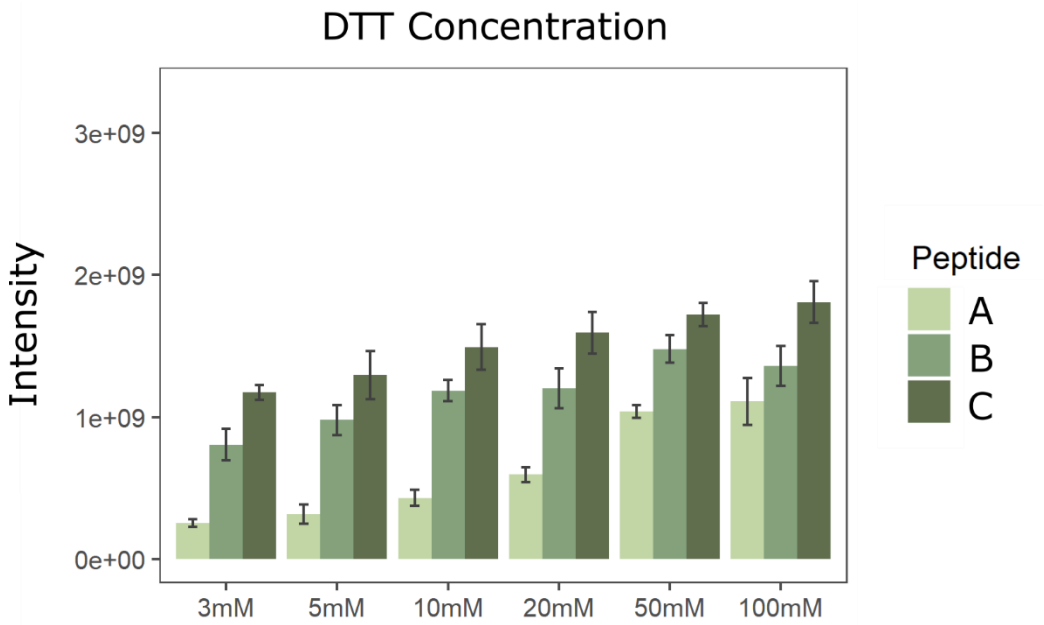

Figure S3: Optimizing the DTT concentration for de-palmitoylation. *For testing the optimal concentration of DTT for de-palmitoylation, the three S-palmitoylated synthetic peptides were mixed and divided into equal volumes. Each sample received one of the following concentrations of DTT; 3mM, 5mM, 10mM, 20mM, 50mM or 100mM. Peptide mix was incubated for 1 hour at room temperature with DTT. The results are average of triplicate experiment.*

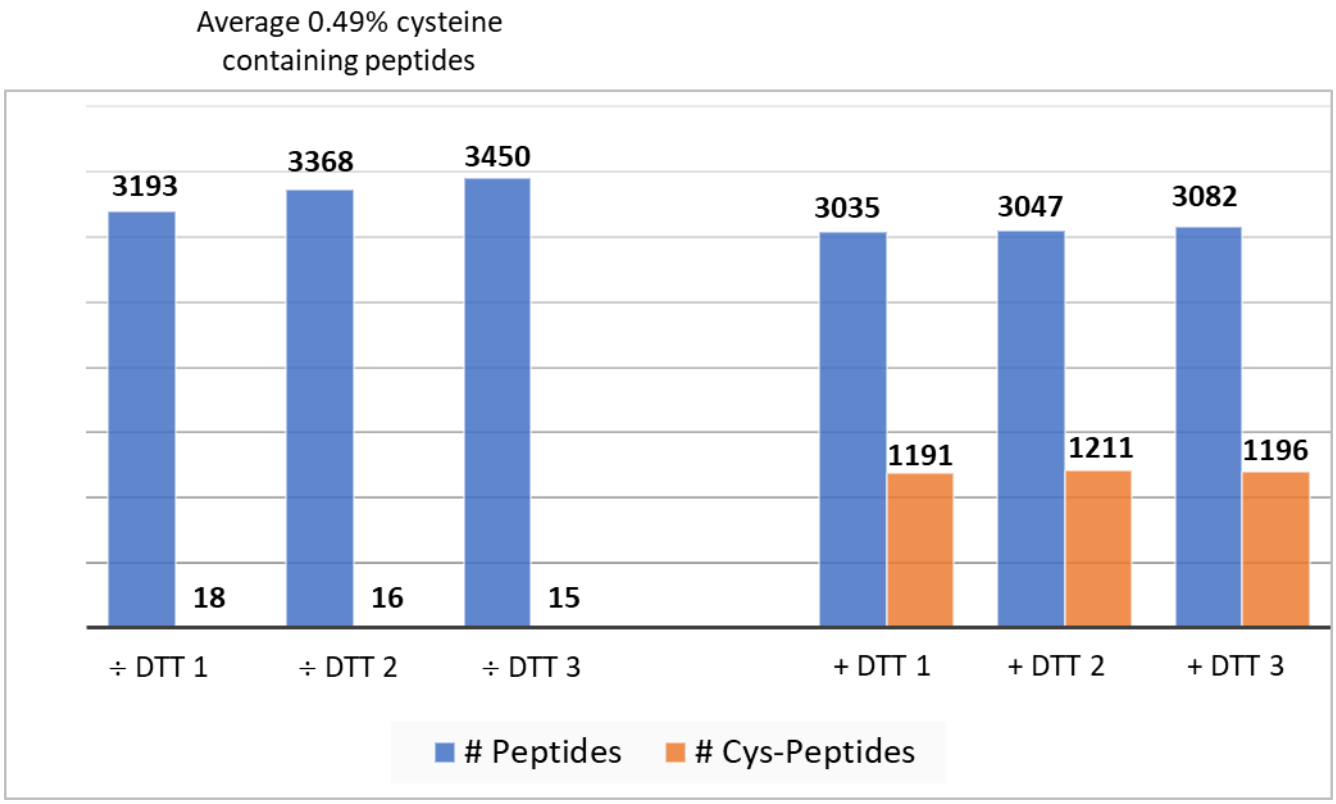

Figure S4: Mouse brain control test with or without DTT. *Aliquots of the mouse brain membrane preparation digested with trypsin in 5% SDC were aliquoted and treated with or without 20mM DTT in triplicates. From the triplicates without DTT (÷ DTT 1-3) only an average of ≈ 0.49 % cysteine containing peptides were identified in the eluate compared to ≈ 39% cysteine containing peptides from the samples with DTT (+ DTT 1-3).*

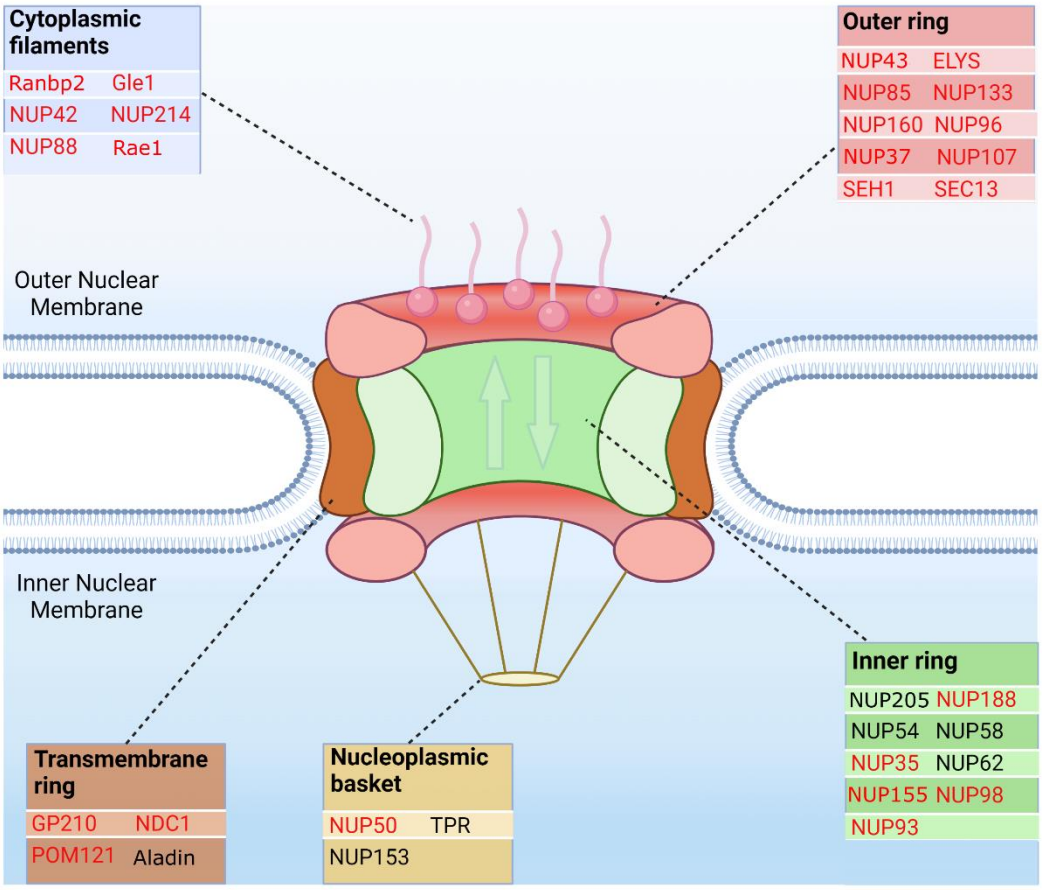

Figure S5: S-palmitoylated components of the nuclear pore complex identified from the mouse brain. *Schematic illustration of the nuclear pore complex architecture that spans the nuclear envelope. Enriched de-palmitoylated peptides from mouse brain could be identified to several proteins (highlighted in red) related to key proteins of the nuclear pore complex. 25 out of the 32 proteins were identified as palmitoylated.*

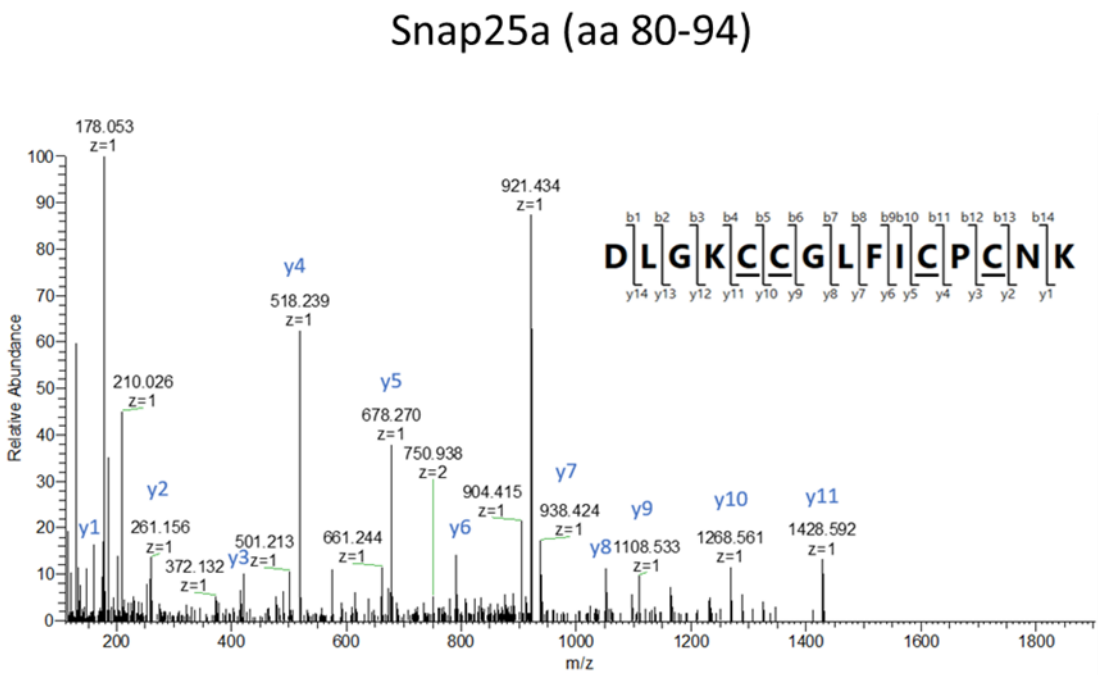

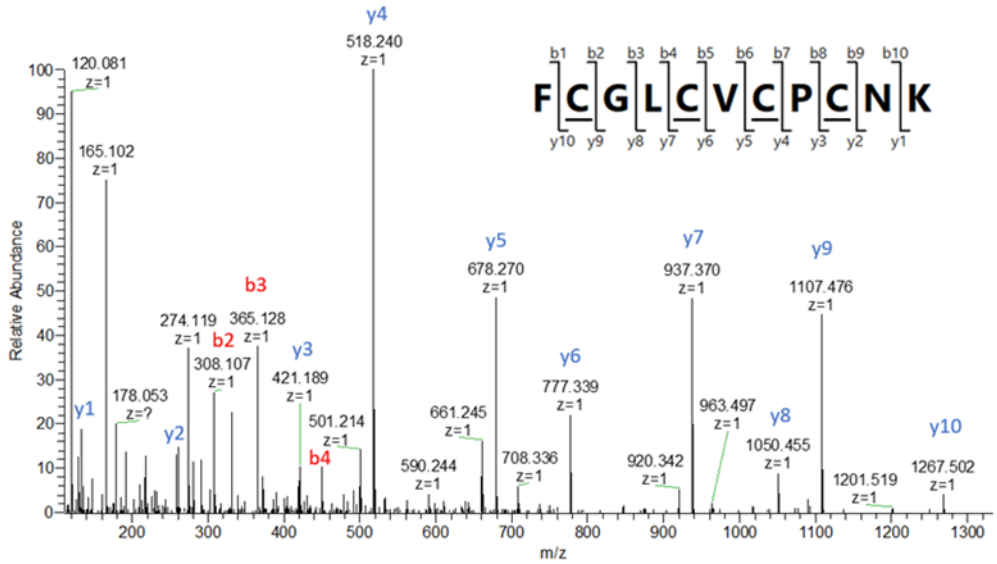

Figure S6: Annotated tandem mass spectra for the peptides containing the S-palmitoylated sites in Snap25 in mouse brains. *A well-known S-palmitoylated protein, Snap25, were identified as S-palmitoylated in both splicing variants (Snap25a and Snap25b). S-palmitoylated sites identified are underscored in the peptide sequence.*

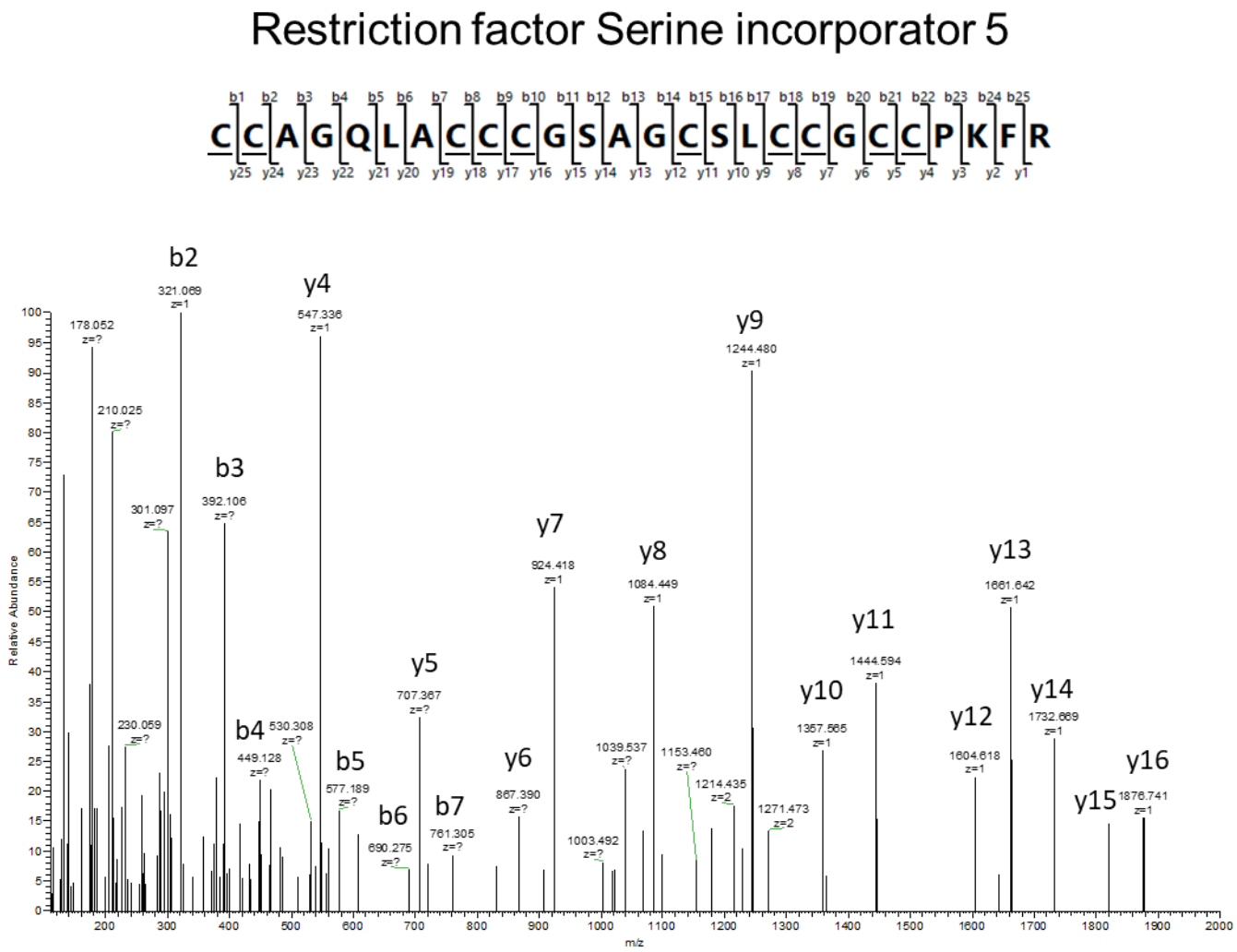

Figure S7: S-palmitoylation of Serine Incorporator 5. *Annotated tandem mass spectrum of a peptide from the Serine Incorporator 5 restriction factor containing 10 S-palmitoylation sites on a single peptide sequence. S-palmitoylated cysteines are underscored in the peptide sequence.*